FED-Vol. 236, 1996 Fluids Engineering Division Conference
Volume 1
ASME 1996

THE EFFECTS OF VAPOR/GAS BUBBLES ON THE ROTORDYNAMIC FORCES IN BEARINGS

Fabrizio d'Auria, Luca d'Agostino
Dipartimento di Ingegneria Aerospaziale
Università degli Studi di Pisa
Pisa, Italy

Christopher E. Brennen
California Institute of Technology
Pasadena, California

ABSTRACT

This paper presents an analytical investigation of the effects that vapor/gas bubbles can have on the fluid-induced rotordynamic forces in a liquid-filled annulus between a cylindrical rotor and a surrounding cylindrical stator. It is demonstrated that such cavitation (vaporous or gaseous) can have important consequences in altering the rotordynamic characteristics of devices such as long journal bearings or long squeeze-film dampers.

A linearized analysis which includes bubble dynamic effects is used to evaluate the rotordynamic effects caused by a small amplitude whirl motion of the rotor in both the high and low Reynolds number regimes of fluid motion. In the former case the Euler equations for a bubbly mixture are employed while, in the latter, a modified Reynolds lubrication equation is used. These are combined with a Rayleigh-Plesset analysis of the bubble dynamics which includes various bubble damping effects. It is shown that, in certain parametric regimes, the normal and tangential fluid-induced rotordynamic forces acting on the rotor can deviate substantially from their classical forms in single-phase flow.

1. INTRODUCTION

The occurrence of cavitation in bearings, its form and contents are strongly dependent on the flow parameters and operating conditions (Dowson and Taylor 1979; Heshmat, 1991). At low angular shaft speeds a localized cavitating zone has been observed to rotate synchronously with the pressure wave (Jacobson and Hamrock 1983, Sun and Brewe 1991). In other circumstances, the liquid in the entire gap appears to transition to a homogeneous two-phase mixture as in the experiments of Walton *et al.* (1986) and Zeidan and Vance (1988) on squeeze-film dampers. In particular, Walton and his coworkers identified different regimes of operation as a function of the shaft angular speed. At lower angular speeds the cavitating zone rotated with the pressure wave. An increase in the angular speed led to the creation of smaller and smaller bubbles capable of surviving the high pressure region of the bearing and invariably leading to the formation of a foamy mixture of oil and air. A number of models for the prediction of the performance of squeeze-film dampers with bubbles in the lubricant have been examined by Feng and Hahn (1987). Contrasting results were obtained, depending on the compressible fluid model used.

The influence of cavitation on whirl instabilities and rotordynamic forces in bearings and seals is a matter of major concern to researchers and designers alike (Childs 1993). Of particular importance is the development of self-sustaining lateral motions (whirl) of the rotating shaft under the action of destabilizing forces (Jery *et al.* 1985; Franz *et al.* 1989, Brennen 1994). For example, in high power density turbopumps, whirl motions can be responsible for very serious problems, ranging from long term fatigue damage to sudden failure of the machine.

The purpose of the present research is to explore the changes in the rotordynamic characteristics of bearings or squeeze film dampers, due to the presence of a dispersed gas in the lubricant. Parenthetically we note that in the related field of cavitating inducers the presence of a bubbly cavitating flow can substantially alter the rotordynamic forces (d'Auria *et al.* 1995).

The unsteady flow in the annulus is studied using the same linear perturbation approach used in previous analyses of the dynamics of bubbly liquids (d'Agostino and Brennen 1983, 1988, 1989; d'Agostino, Brennen and Acosta 1988; Kumar and Brennen 1993). In spite of the intrinsic limitations of the linear approximation and the simplifying assumptions introduced in order to obtain a closed form solution, the present analysis identifies some of the basic features of the dynamics of a bubbly flow in the annulus between two cylinders.

2. DYNAMICS OF A BUBBLY FLOW SURROUNDING A WHIRLING CYLINDER

Consider the flow in an annulus between two cylinders, as sketched in Figure 1. The inner cylinder or "rotor" (rotating reference frame O', r', ϑ'), of radius a, rotates with angular speed, Ω, and performs a circular whirl motion of frequency, ω, and assigned eccentricity, ε.

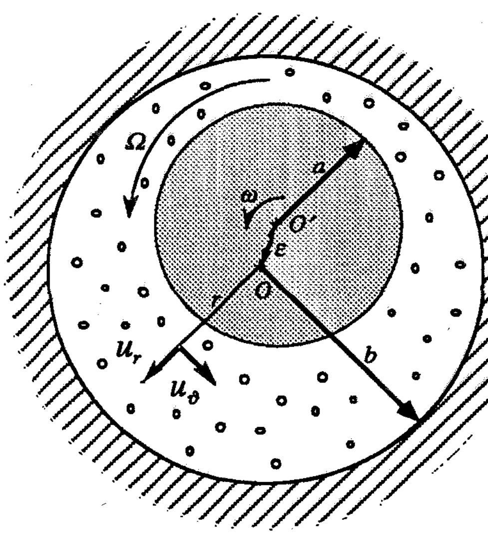

Figure 1. Schematic illustrating rotor whirl and rotation.

The annulus (absolute reference frame O,r,ϑ) contains a liquid with uniformly dispersed spherical bubbles. A key parameter of the fluid is the population of bubbles, β, per unit liquid volume which, neglecting relative motion and the mass of liquid vaporized, will remain constant. We address the problem of finding the fluid-induced rotordynamic forces acting on the rotor.

2.1. High Reynolds Number Approximation

Basic Equations

Consider an inviscid liquid containining a population of spherical bubbles of radius, R. The continuity, momentum and Rayleigh-Plesset equations for the bubbly mixture, neglecting relative motion between the two phases and assuming that no bubbles are created or destroyed, can be written as (d'Agostino and Brennen, 1988):

$$\nabla\cdot\boldsymbol{u}=\frac{\alpha}{\tau}\frac{D\tau}{Dt} \tag{1}$$

$$\rho_L(1-\alpha)\frac{D\boldsymbol{u}}{Dt}=-\nabla p \tag{2}$$

$$\begin{aligned}&\left(1-\frac{\dot R}{c_L}\right)R\ddot R+\frac{3\dot R^2}{2}\left(1-\frac{\dot R}{3c_L}\right)=\\&=\left(1+\frac{\dot R}{c_L}\right)\frac{p_R(t)-p(t+R/c_L)}{\rho_L}+\frac{R}{\rho_L c_L}\frac{dp_R(t)}{dt}\end{aligned} \tag{3}$$

where $D/Dt=\partial/\partial t+\boldsymbol{u}\cdot\nabla$ indicates the Lagrangian time derivative following the liquid, $\tau=4\pi R^3/3$ is the volume of the bubbles, p is the pressure, ρ_L is the liquid density, μ_L is the liquid viscosity, c_L is the speed of sound in the liquid, and α is the void fraction, related to the bubble population, β, by $\alpha=\beta\tau/(1+\beta\tau)$. In the last equation, dots denote Lagrangian time derivatives following the bubbles, and $p_R(t)$ is the liquid pressure at the bubble surface, related to the bubble internal pressure p_B (assumed uniform and consisting of vapor and non-condensable gas partial pressures) by:

$$p_B(t)=p_R(t)+\frac{2S}{R}+4\mu_L\frac{\dot R}{R} \tag{4}$$

where S is the surface tension of the bubble interface. Clearly, for the closure of the problem, the above equations must be supplemented by the mechanical and thermal equations of state and by the energy conservation equations for the two phases with the relevant boundary and matching conditions (d'Agostino and Brennen, 1988).

Linearization and Perturbation Flow

It is convenient to analyze the flow in a Lagrangian frame, r_L,ϑ_L, moving with the fluid, and to define $\omega_L=\Omega_o-\omega$ as the frequency of excitation in this Lagrangian frame where Ω_0 is some representative angular velocity of the mean flow which, for very small clearances can be approximated as $\Omega_o\approx\Omega/2$. Having defined an unperturbed equilibrium flow (denoted by subscript o) one can then examine linearized perturbations of frequency ω_L. This yields the following Helmholtz equation (d'Agostino and Brennen 1988):

$$\nabla^2\hat p+k^2(\omega_L)\hat p=0 \tag{5}$$

where $\hat p$ is the complex amplitude of the pressure fluctuation, $\tilde p$, so that $\tilde p=\mathrm{Re}\{\hat p e^{-i\omega_L t}\}$, where $\mathrm{Re}\{\ \}$ denotes the real part. From the momentum equation (2), the velocity and pressure perturbations are related by $i\omega_L\rho_L(1-\alpha)\hat{\boldsymbol{u}}=\nabla\hat p$. It transpires that the free-space wave number, k, is determined by the dispersion relation:

$$\frac{1}{c_M^2(\omega_L)}=\frac{k^2(\omega_L)}{\omega_L^2}\approx\frac{1}{c_{Mo}^2}\left(\frac{\omega_{Bo}^2}{\omega_B^2-\omega_L^2-i\omega_L 2\lambda}\right) \tag{6}$$

Here $c_M(\omega_L)$ is the complex and dispersive (frequency dependent) speed of propagation of harmonic disturbances of angular frequency ω_L in the free bubbly mixture, and $\omega_B(\omega_L)$ and $\lambda(\omega_L)$ are the effective natural frequency and damping coefficient of an individual bubble when excited at frequency ω_L (Plesset and Prosperetti 1977). Also:

$$\omega_{Bo}^2=\frac{3p_o}{\rho_L R_o^2}-\frac{2S}{\rho_L R_o^3}\quad\text{and}\quad c_{Mo}^2=\frac{\omega_{Bo}^2R_o^2}{3\alpha(1-\alpha)} \tag{7}$$

where ω_{Bo} is the natural frequency of oscillation of a single bubble at isothermal conditions in an unbounded liquid with pressure p_o and c_{Mo} is the low-frequency sound speed in a free bubbly flow with incompressible liquid ($\omega_L\to0$ and $c\to\infty$). Notice that the propagation speed and wave number depend on the radial coordinate through the mean pressure p_o, thereby making the Helmholtz equation quasi-linear.

By separation of variables the solution for the pressure perturbation is readily expressed in terms of the Bessel functions J_1 and Y_1 and their derivatives (d'Auria *et al.* 1995):

$$p-p_o=\mathrm{Im}\left[i\varepsilon b\omega_L{}^2\rho_L(1-\alpha)G(r,\omega_L)\exp\{i(\vartheta-\omega t)\}\right]$$

where $\mathrm{Im}\{\ \}$ denotes the imaginary part and the function $G(r,\omega_L)$ has the following form:

$$G(r,\omega_L)=\frac{1}{kb}\frac{J_1(kr)Y_1'(kb)-Y_1(kr)J_1'(kb)}{J_1'(ka)Y_1'(kb)-Y_1'(ka)J_1'(kb)},\qquad k=\left(k^2(\omega_L)\right)^{1/2}$$

The contribution of the pressure perturbation to the fluid-induced rotordynamic forces can then be computed as will be described below.

2.2. The Low Reynolds Number Approximation

The Reynolds Lubrication Equation for a Bubbly Mixture

We now turn attention to the other limit of low Reynolds number flow in the annulus. The appropriate Reynolds lubrication equation for a single phase flow (Sherman 1990) is:

$$\nabla\cdot\left[\left(\frac{\rho h^3}{\mu}\right)\nabla p\right]=12\frac{\partial(\rho h)}{\partial t}+6\nabla\cdot(\rho hU) \tag{8}$$

The local spacing between the rotor and stator is denoted by h, p is the pressure in the annulus and U is the relative speed between the two surfaces. In the present context the fluid density, $\rho=\rho_L(1-\alpha)$, and the void fraction, α, will vary in space and time, the void fraction being given by the bubble radius which is, in turn, given by the Rayleigh-Plesset equation.

As in the previous analyses we examine the linearized perturbation solution for this system of equations denoting the complex amplitude function by the hat accent. Then the Rayleigh-Plesset equation yields:

$$\hat{R}=\eta\hat{p} \tag{9}$$

where

$$\eta=-\frac{1}{\rho_L R_o\left(\omega_B^2-\omega_L^2-i\omega_L 2\lambda\right)}$$

Solving the linearized Reynolds equation for the pressure perturbation, $\tilde{p}=\mathrm{Re}\left\{\hat{p}\exp[i(\omega t-\vartheta)]\right\}$, we obtain:

$$\tilde{p}=-\mathrm{Re}\left\{\frac{\rho_L\varepsilon a^2\omega_L^2/h_o^2}{k^2a^2-\dfrac{\mathrm{Re}_L}{12i}}\exp\{i(\omega t-\vartheta)\}\right\} \tag{10}$$

where k is the previously defined wave number and $\mathrm{Re}_L=\omega_L h_o^2\rho_L/\mu_L$ is the Reynolds number based on the Lagrangian frequency, ω_L. In the derivation of the Reynolds equation it is assumed that $\mathrm{Re}_L<<1$, namely that viscous forces dominate the phenomenon. In the absence of a dispersed phase in the liquid ($\alpha=k=0$), the usual linearized expression for the pressure perturbation in a journal bearing is recovered (Pinkus and Sternlicht 1961).

The Reynolds Lubrication Equation for a Bubbly Mixture including Inertial Effects

We can include small inertial effects in the low Reynolds number analysis by following the approach of Sherman (1990). The continuity and momentum equations for the lubricant can be written as follows:

$$\frac{\partial(\rho h)}{\partial t}+\nabla\cdot(\rho h\boldsymbol{u})=0$$

$$\boldsymbol{u}=U-\frac{h^2}{12\mu}\left\{\nabla p+\rho\left[\frac{\partial\boldsymbol{u}}{\partial t}+(\boldsymbol{u}\cdot\nabla)\boldsymbol{u}\right]\right\}$$

The above equations are then linearized following the procedure described above. Solving for the pressure perturbation yields:

$$\tilde{p}=-\mathrm{Re}\left\{\frac{\rho_L\varepsilon a^2\omega_L^2(1-\mathrm{Re}_L/12i)/h_o^2}{k^2a^2\left(1-\dfrac{\mathrm{Re}_L}{12i}\right)-\dfrac{\mathrm{Re}_L}{12i}}\exp\{i(\omega t-\vartheta)\}\right\} \tag{11}$$

Notice that equation (10) can be recovered from equation (11) when $\mathrm{Re}_L<<1$, that is when inertial effects are neglected when compared to viscous effects. Again notice that the deviations from the linearized solution of the Reynolds lubrication equation for a single phase flow (Brennen 1994) are given by the terms in the wave number k. We shall also present results for this modified low Reynolds number analysis.

3. ROTORDYNAMIC FORCES

The fluid-induced rotordynamic forces per unit length of the rotor are obtained by means of the following relations (Brennen 1994):

$$f_N=-a\int_0^{2\pi}p\cos(\omega t-\vartheta)d\vartheta\quad,\quad f_T=a\int_0^{2\pi}p\sin(\omega t-\vartheta)d\vartheta \tag{12}$$

and it is convenient to define nondimensional forces per unit length as follows:

$$f_N^*=f_N/\pi\varepsilon\rho\Omega^2b^2\quad,\quad f_T^*=f_T/\pi\varepsilon\rho\Omega^2b^2$$

4. RESULTS AND DISCUSSION

The following results are obtained for the case of a rotor whirling in an ideal fluid having viscosity in the range $\mu=0.005\to0.05\ \mathrm{Ns/m^2}$.

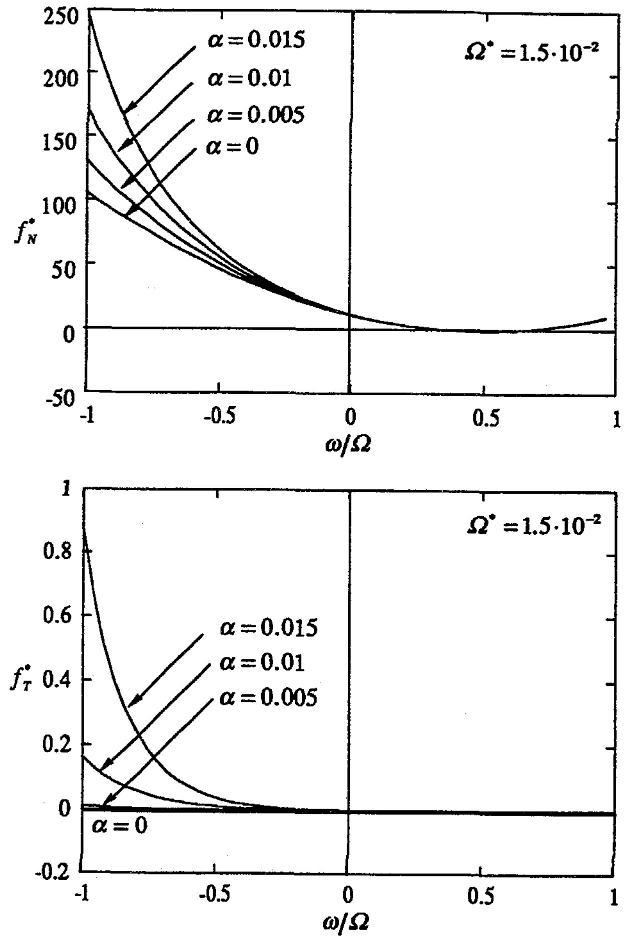

Figure 2. Inviscid Formulation. $\Omega^*=1.5\cdot10^{-2}$. Normal and tangential rotordynamic forces per unit length, f_N^* and f_T^*, as a function of the whirl ratio, ω/Ω, for $\alpha=0.005$, $\alpha=0.01$, $\alpha=0.015$, and single-phase flow. In all cases $R^*=10^{-1}$ and $h_o^*=7.5\cdot10^{-3}$. $\mu=0.005$ Ns/m^2.

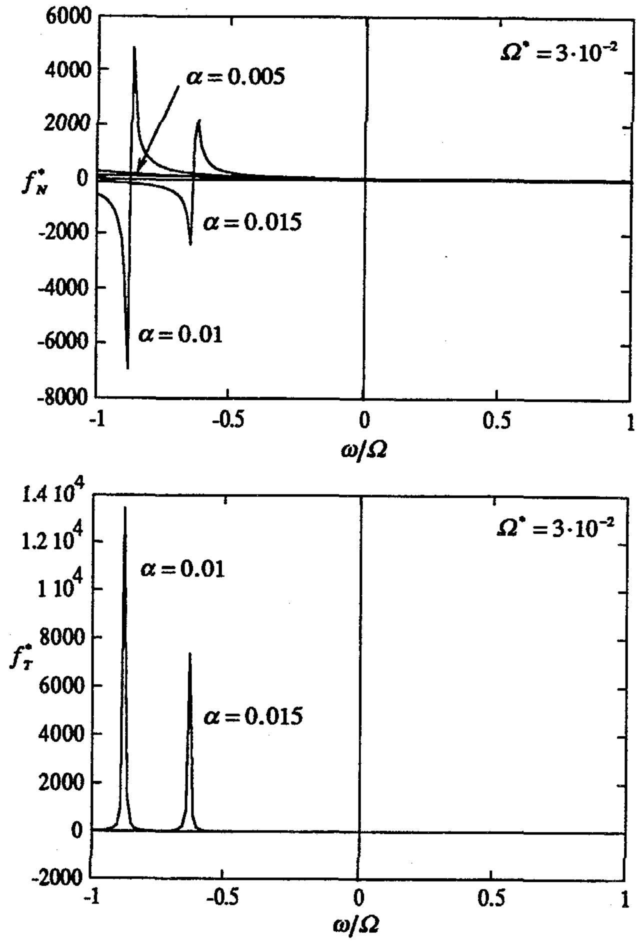

Figure 3. Inviscid Formulation. $\Omega^*=3\cdot10^{-2}$. Normal and tangential rotordynamic forces per unit length, f_N^* and f_T^*, as a function of the whirl ratio, ω/Ω, for $\alpha=0.005$, $\alpha=0.01$, $\alpha=0.015$, and single-phase flow. In all cases $R^*=10^{-1}$ and $h_o^*=7.5\cdot10^{-3}$, $\mu=0.005$ Ns/m^2.

The nondimensional parameters for this flow are the mean void fraction, α, the mean bubble radius, $R^*=R/(b-a)$, the mean clearance $h_o^*=(b-a)/a$, and the angular velocity expressed by the Reynolds number, defined as $\mathrm{Re}=\Omega h_o^2\rho_L/\mu_L$ (Muster and Sternlicht 1965), in the viscous formulation, and by $\Omega^*=\Omega/\omega_{B_o}$ in the inviscid formulation. First consider the inviscid or high Reynolds number formulation of the problem. In this case Figures 2 and 3 show the effect of the whirl ratio, ω/Ω, on the normal and tangential forces per unit length, f_N^* and f_T^*, for different values of the void fraction and for two different values of Ω^*. As the void fraction increases, appreciable deviations from the quadratic behavior of the non-cavitating flow ($\alpha=0$) can be observed. At higher rotor speed, Ω^*, sign inversions of the normal force, f_N^*, are also possible. Notice that the inviscid formulation results in extremely high peaks in the forces.

The presence of a dispersed gaseous phase in the liquid also results in a non-zero tangential force, f_T^*, even in the inviscid formulation.

Now consider the Reynolds lubrication solution. Contrary to the inviscid formulation, which was dominated by inertial effects, viscous forces are now dominant. Figures 4 and 5 show the behavior of the normal and tangential forces per unit length, f_N^* and f_T^*, as a function of the whirl ratio, ω/Ω, for two values of the Reynolds number, Re, and for different values of the void fraction. In the absence of bubbles this model would predict zero normal force but the presence of the dispersed phase results in a non-zero normal force. It can be observed that the normal force increases with the void fraction. Notice that the presence of bubbles in the liquid results in a value of the normal force having the same order of magnitude as the tangential force.

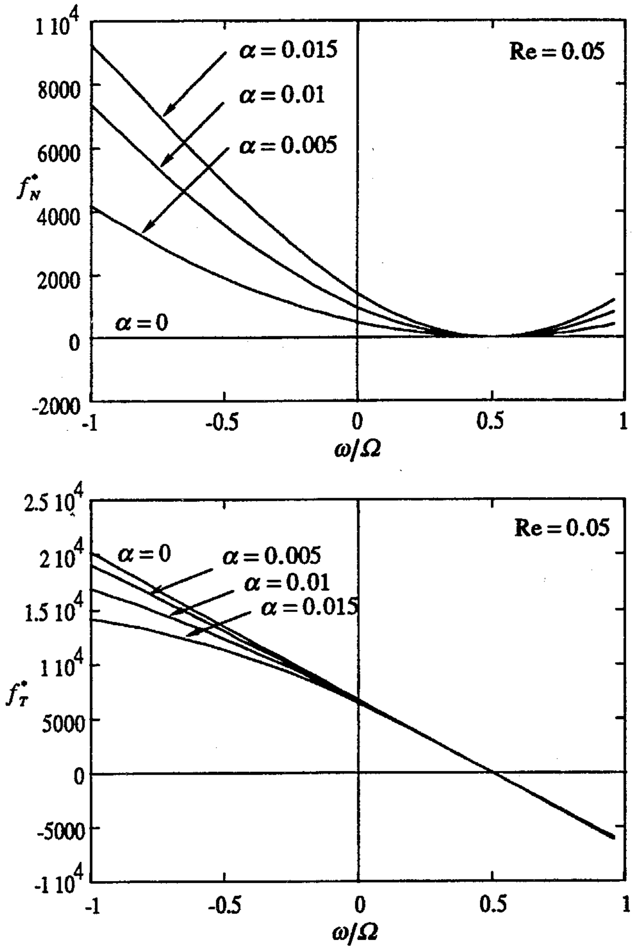

Figure 4. Reynolds Approximation, $\mathrm{Re} = 0.05$. Normal and tangential rotordynamic forces per unit length, f_N^* and f_T^*, as a function of the whirl ratio, ω/Ω, for $\alpha = 0.005$, $\alpha = 0.01$, $\alpha = 0.015$, and single-phase flow. In all cases $R^* = 10^{-1}$ and $h_o^* = 7.5 \cdot 10^{-3}$, $\mu = 0.05\ \mathrm{Ns/m^2}$.

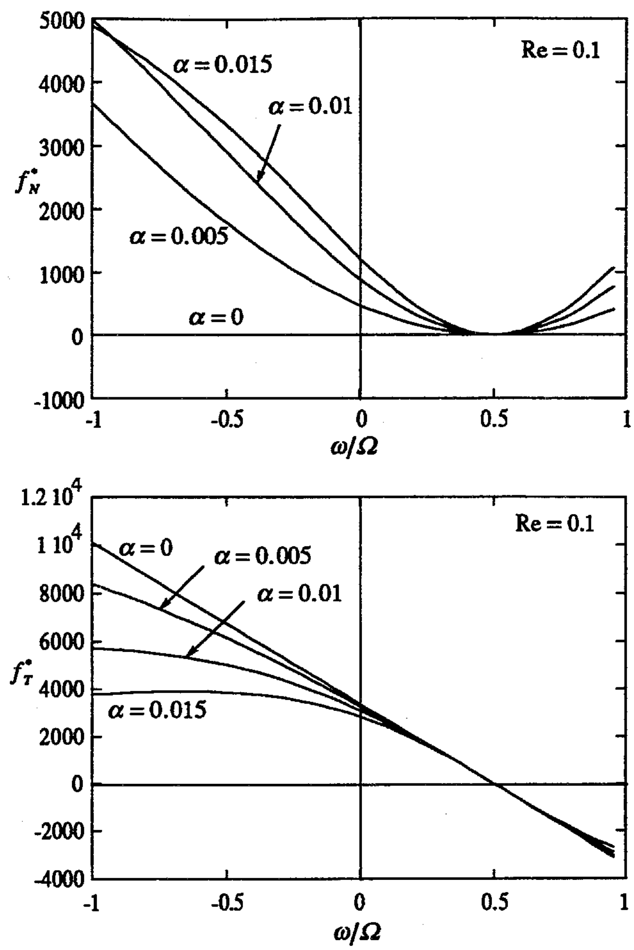

Figure 5. Reynolds Approximation, $\mathrm{Re} = 0.1$. Normal and tangential rotordynamic forces per unit length, f_N^* and f_T^*, as a function of the whirl ratio, ω/Ω, for $\alpha = 0.005$, $\alpha = 0.01$, $\alpha = 0.015$, and single-phase flow. In all cases $R^* = 10^{-1}$ and $h_o^* = 7.5 \cdot 10^{-3}$, $\mu = 0.05\ \mathrm{Ns/m^2}$.

Its qualitative behavior is substantially unaffected by a variation in the Reynolds number, Re. The tangential force, f_T^*, decreases with the void fraction, in the negative whirl region. This effect gets stronger as Re increases. The magnitudes of both f_N^* and f_T^* decrease with Re.

Finally consider the Reynolds equation for the bubbly mixture with the addition of inertial effects. Figures 6 and 7 show the normal and tangential force per unit length, f_N^* and f_T^*, for sufficiently high values of *Re* so that the behavior of inertial effects can be observed. Notice that at lower values of Re (Fig. 6) the behavior of the normal force, f_N^*, is qualitatively similar to that obtained from the solution of the Reynolds lubrication equation without inertial effects (see, for example, Fig. 4). As Re increases (Fig. 7), substantial inertial effects are evident. Notice that the computed behavior is consistent with that observed in the inviscid formulation, thus confirming physical trends obtained with a completely different mathematical model.

Obviously, the strong peaks of the forces in the inviscid formulation (see Figure 3) are now damped by viscous effects. Similar remarks are in order when observing the behavior of the tangential forces, f_T^*. Inertial effects clearly dominate the tangential forces and those effects are significantly altered by the bubbles.

In summary, the presence of a dispersed phase in the liquid film can induce substantial modifications to the rotordynamic forces on the rotor. The magnitude and nature of these modifications are strongly dependent on the void fraction and on the Reynolds number.

5. CONCLUSIONS

The purpose of this paper has been to explore the changes in the rotordynamic characteristics of bearings or squeeze film dampers, due to the presence of a dispersed gas in the lubricant.

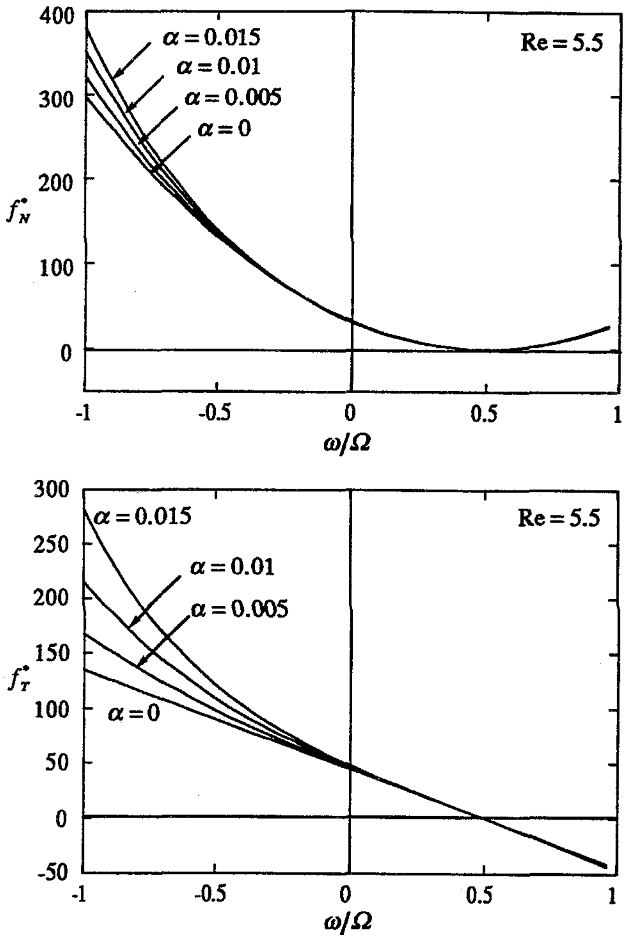

Figure 6. Reynolds Approximation with Inertial Effects, $Re = 5.5$. Normal and tangential rotordynamic forces per unit length, f_N^* and f_T^*, as a function of the whirl ratio, ω/Ω, for $\alpha = 0.005$, $\alpha = 0.01$, $\alpha = 0.015$, and single-phase flow. In all cases $R^* = 10^{-1}$ and $h_o^* = 7.5 \cdot 10^{-3}$, $\mu = 0.005$ Ns/m^2.

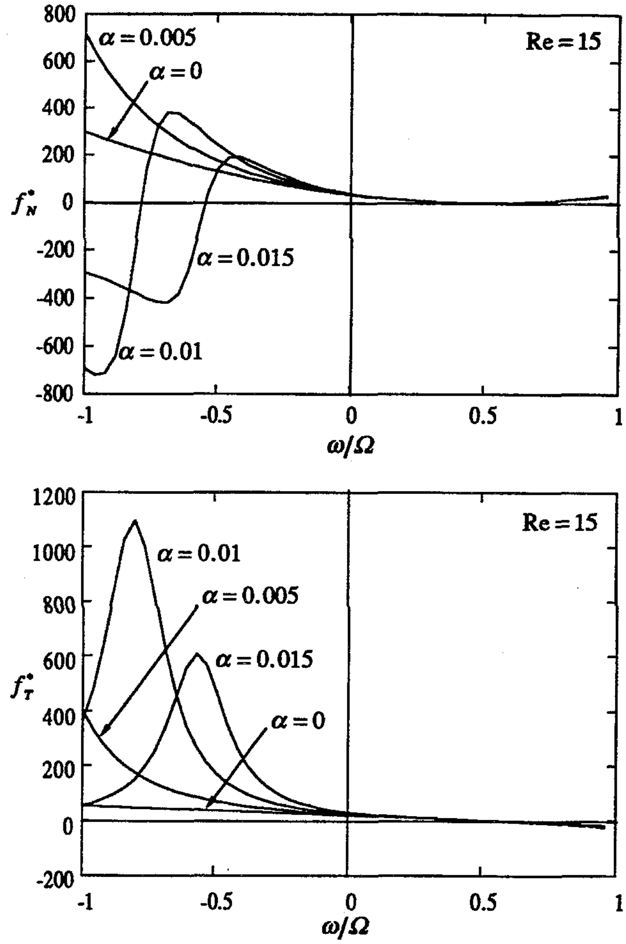

Figure 7. Reynolds Approximation with Inertial Effects, $Re = 15$. Normal and tangential rotordynamic forces per unit length, f_N^* and f_T^*, as a function of the whirl ratio, ω/Ω, for $\alpha = 0.005$, $\alpha = 0.01$, $\alpha = 0.015$, and single-phase flow. In all cases $R^* = 10^{-1}$ and $h_o^* = 7.5 \cdot 10^{-3}$, $\mu = 0.005$ Ns/m^2.

The results of this study reveal a number of substantial effects on the fluid-induced rotordynamic forces in a liquid-filled annulus between a cylindrical rotor and a surrounding cylindrical stator as a consequence of the strong coupling between the local dynamics of the bubbles and the global behavior of the flow.

The propagation of the whirl-induced disturbances within the annulus is significantly modified by the large reduction in the sonic speed and the specific geometry of the flow. As a consequence of these modifications, the rotordynamic fluid forces on the whirling shaft have a complex dependence on the whirl frequency. The high and low Reynolds number approximations, based on quite different mathematical models yield qualitatively consistent behaviors.

The present exploratory analysis has focused on the effect of the whirl ratio and void fraction on the fluid-induced forces. Results show that such forces are strongly dependent on both of these parameters; the Reynolds number (and its related variables) still remains to be systematically investigated.

The present theory is based upon fairly restrictive assumptions and, therefore, is not expected to provide a quantitative description of unsteady bubbly flows in bearings. Nonetheless we hope that it will contribute to a better physical understanding of rotordynamic phenomena in bearings and squeeze film dampers.

6. ACKNOWLEDGMENTS

This work has been supported by the Italian Ministry of Universities and Scientific Research and by the Office of Naval Research under grant number N-00014-91-K-1295.

REFERENCES

Brennen, C. E., 1994, "Hydrodynamics of Pumps", Concepts ETI Inc. and Oxford University Press.

Brennen, C. E., 1995, "Cavitation and Bubble Dynamics", Oxford University Press

Ceccio, S.L., and Brennen, C.E., 1990, "Observations of the Dynamics and Acoustics of Attached Cavities", *ASME Cavitation and Multiphase Flow Forum*, Toronto, Ontario, Canada, pp. 79-84.

Childs, D., 1993, "Turbomachinery Rotordynamics; Phenomena Modeling and Analysis", Wiley Interscience Publications.

d'Agostino, L., and Brennen, C.E., 1983, "On the Acoustical Dynamics of Bubble Clouds", *ASME Cavitation and Multiphase Flow Forum*, Houston, Texas.

d'Agostino, L., and Brennen, C.E., 1988, "Acoustical Absorption and Scattering Cross-Sections of Spherical Bubble Clouds", *J. Acoust. Soc. Am.*, No. 84 (6), pp. 2126-2134.

d'Agostino, L., and Brennen, C.E., 1989, "Linearized Dynamics of Spherical Bubble Clouds", *J. Fluid Mech.*, Vol. 199, pp. 155-176.

d'Agostino, L., Brennen, C.E., and Acosta, A.J., 1988, "Linearized Dynamics of Two-Dimensional Bubbly and Cavitating Flows over Slender Surfaces", *J. Fluid Mech.*, Vol. 192, pp. 485-509.

d'Auria, F., d'Agostino, L., and Brennen, C.E., 1995, "Bubble Dynamics Effects on the Rotordynamic Forces in Cavitating Inducers", *ASME Cavitation and Multiphase Flow Forum*, FED-Vol. 210, pp. 47-54, Hilton Head Island.

Dowson, D., and Taylor, C. M., 1979, "Cavitation in Bearings", *Ann. Rev. Fluid Mech.*, Vol. 11, pp. 35-66.

Feng, N. S., and Hahn, E. J., 1987, "Effects of Gas Entrainment on Squeeze Film Damper Performance", *ASME J. of Tribology*, Vol. 109, pp. 149-154.

Franz, R., Acosta, A.J., Brennen, C.E., and Caughey, T.K., 1990, "The Rotordynamic Forces on a Centrifugal Pump Impeller in the Presence of Cavitation", *ASME J. Fluids Eng.*, Vol. 112, pp. 264-271.

Greitzer, E.M., 1980, "The Stability of Pumping Systems", *ASME J. Fluids Eng.*, Vol. 103, pp. 193-242.

Heshmat, H., 1991, "The Mechanism of Cavitation in Hydrodynamic Lubrication", STLE Tribology Transactions, Vol. 34, pp. 177-186

Jacobson, B. O., and Hamrock, B. J., 1983, "High-Speed Motion Picture Camera Experiments of Cavitation in Dynmically Loaded Journal Bearings", *ASME J. Lubrication Technology*, Vol. 105, pp. 446-452.

Jery, B., Brennen, C.E., Caughey, T.K., and Acosta, A.J., 1985, "Forces on Centrifugal Pump Impellers", *2nd Int. Pump Symp.*, Houston, Texas, April 29-May 2, 1985.

Knapp, R. T., Daily, J. W., and Hammit, F. G., 1970, "Cavitation", *McGraw Hill*, New York.

Kumar, S., and Brennen, C.E., 1993, "Some Nonlinear Interactive Effects in Bubbly Clouds", *J. Fluid Mech.*, Vol. 253, pp. 565-591.

Pinkus, O., and Sternlicht, B., 1961, "Theory of Hydrodynamic Lubrication", *Mc Graw-Hill*, NewYork.

Muster, D., and Sternlicht, B., 1965, "Proceedings of the International Symposium on Lubrication and Wear", *McCutchan Publishing Co.*, Berkeley.

Plesset, M. S., and Prosperetti, A., 1977, "Bubble Dynamics and Cavitation", *Ann. Rev. Fluid. Mech.*, Vol. 9, pp. 145-185.

Prosperetti, A., 1977, "Thermal Effects and Damping Mechanisms in the Forced Radial Oscillations of Gas Bubbles in Liquids", *J. Acoust. Soc. Am.*, Vol. 61, No. 1 (6), pp. 17-27.

Prosperetti, A., 1984, "Bubble Phenomena in Sound Fields: Part One", *Ultrasonics*, March 1984, pp. 69-78.

Sherman, F., 1990, "Viscous Flow", *McGraw-Hill Inc.*, New York.

Sun, D. C., and Brewe, D. E., 1991, "A High-speed Photography Study of Cavitation in a Dynamically Loaded Journal Bearing", *ASME J. of Tribology*, Vol. 113, pp. 287-294.

Sun, D. C., Brewe, D. E., and Abel, P. B., 1993, "Simultaneous Pressure Measurement and High-speed Photography Study of Cavitation in a Dynamically Loaded Journal Bearing", *ASME J. of Tribology*, Vol. 115, pp. 88-95.

Walton II, J. F., Walowit, J.A., Zorzi, E.S., Schrand, J., 1987, "Experimental Observation of Cavitating Squeeze-Film Dampers", *Trans. ASME J. Tribology* Vol.109, pp. 290-295.

Zeidan, F.Y., and Vance, J.M., 1989, "Cavitation Leading to a Two-Phase Fluid in a Squeeze Film Damper", *STLE Tribology Trans.*, Vol. 39, pp.100-104.